PNAS
www.pnas.org

Supplementary Information for

FcαRI binding at the IgA1 C_H2-C_H3 interface induces long-range conformational changes that are transmitted to the hinge region

Monica T. Posgai, Sam Tonddast-Navaei, Manori Jayasinghe, George M. Ibrahim, George Stan, and Andrew B. Herr

Correspondence: George Stan
Email: george.stan@uc.edu
Correspondence: Andrew B. Herr
Email: andrew.herr@cchmc.org

This PDF file includes:

Supplementary text
Figs. S1 to S7
Tables S1 to S4
Captions for movies SM1 to SM15
References for SI reference citations

Other supplementary materials for this manuscript include the following:

Movies SM1 to SM15

Supplementary Methods

Circular Dichroism

Far-UV CD experiments were carried out at 25 ºC in an Aviv 215 circular dichroism spectrometer using 0.5 mm quartz cuvettes. Wavelength scans were performed from 260-185 nm with 1 nm steps. Data were collected in triplicate on Fcα wildtype and variant proteins, at concentrations ranging from 0.462 to 1.172 mg/mL, in buffer containing 0.02 M sodium phosphate, pH 7.4. Units were converted from millidegrees to mean residue ellipticity and spectra from 190-240 nm were deconvoluted using reference set 4 of the CDSSTR algorithm in the Dichroweb program (http://www.cryst.bbk.ac.uk) (1, 2). Average error values were converted to mean residue ellipticity as described (3).

IgA1 C_H3 cloning, expression, refolding, and purification

Using the Fcα-pcDNA3 plasmid as a template, PCR was used to amplify residues Ser341-Lys450 encoding the C_H3 domain of IgA1 (Cα3), and insert an upstream tobacco vein mottling virus cleavage site (ETVRFQG). The PCR product was cloned into the Gateway pDEST17 vector containing an N-terminal His-tag (Invitrogen, Carlsbad, CA). Correct sequence was confirmed by DNA sequencing. Tuner (DE3) pLysS cells were induced overnight with 1 mM IPTG for robust expression of Cα3 protein in inclusion bodies, confirmed by Western blot. Cells were lysed by sonication and inclusion body pellets were washed and solubilized overnight in buffer containing 6 M GdnHCl, 0.5 M NaCl, 0.02 M NaH_2PO_4, and 0.01 M imidazole. Following HisTrap purification under denaturing conditions, 10 mL of 1 mg/mL reduced denatured Cα3 was dialysis refolded in 500 mL of dialysate containing 0.5 M L-arginine HCl, 0.1 M Tris-HCl, pH 7.4, 0.001 M EDTA, 0.45% (w/v) Cyclofos-4, 0.005 M oxidized glutathione, 0.0005 M reduced glutathione). Over a period of 7 days, dialysate was changed to 0.02 M Tris-HCl, pH 7.4, 0.15 M NaCl by gradual decreases in urea, then arginine, followed by Cyclofos-4. Refolded Cα3 was purified by size chromatography using a Hi Load 26/60 Superdex 75 prep grade column (GE Healthcare). Protein purity was determined to be >95% by SDS-PAGE.

Analytical ultracentrifugation

To determine whether the purified refolded Cα3 protein formed homodimers in solution, analytical ultracentrifugation sedimentation velocity experiments were carried out at 20 °C using a Proteome Lab XL-I analytical ultracentrifuge (Beckman Coulter, Indianapolis, IN). Refolded Cα3 protein was sedimented at 48,000 rpm overnight. For sedimentation velocity experiments, 400 μL samples in 0.02 M Tris-HCl, pH 7.4, and 0.15 M NaCl were centrifuged overnight at 48,000 rpm at 20 °C in a Beckman XL-I using absorbance optics at 280 nm. The data were analyzed by the program Sedfit using the c(s) and c(m) models to determine differential sedimentation coefficient and apparent mass distributions, respectively. Cα3 sedimented primarily as a single peak, with a sedimentation coefficient of 2.28 S and an estimated molecular mass of 25.8 kDa, similar to that expected for a homodimer (28.6 kDa).

Biosensor Analysis

BIAcore CM5 chip surfaces were prepared for coupling by pre-conditioning to decrease noise and increase sensitivity (4) (2 sequential 50 μL pulses at 100 μL/min of: 0.05 M NaOH, 0.01 M HCl, 0.1% SDS, and 0.085% H_3PO_4), followed by signal normalization between flow cells. Fcα variants were immobilized by standard random-amine chemistry. Ligands (wildtype or mutant Fcα) in PBS were diluted to 5 μg/mL in 10 mM sodium acetate buffer pH 5.0, injected at 5 μL/min, and immobilized to ~200 response units (RU). We previously demonstrated that random-amine and oriented capturing produced equivalent binding data (5). The response of a mock-coupled flow cell was subtracted to correct for non-specific interaction of the analyte (soluble FcαRI ectodomain) with the chip surface, followed by subtraction of a buffer injection. Each chip also contained a control flow cell immobilized with wildtype Fcα to monitor for variations among chips, confirm accurate analyte concentration, and allow for direct comparison of Fcα mutants between chips.

For equilibrium binding experiments, binding curve alignment and buffer blank subtraction were performed with BIAeval 4.1 software (GE Healthcare). The program Scrubber 2.0 (BioLogic Software, Campbell, Australia) was used to generate initial binding isotherms by averaging the response over a 15-second window at equilibrium. Equilibrium data were fitted globally in the program Scientist 3.0 (Micromath, Saint Louis, MO) to a single-site or a bivalent ligand binding model to determine K_D1 and K_D2, the binding affinity of the first and second binding events. For the two Fcα mutants with the greatest decreases in affinity (L258A and F443A), binding isotherms did not approach saturation, requiring the plateau values to be fixed at levels corresponding to binding curves from other Fcα variants. The one-site and two-site binding model fits were statistically compared using F-ratio statistics (1),

$$F = \frac{(SS1 - SS2)/SS2}{(DF1 - DF2)/DF2}, \quad (1)$$

where SS is the sum of the squared deviations of the fitted experimental data, and DF is the degrees of freedom (data points minus fitted parameters) of the binding model, with '1' and '2' indicating a one-site or two-site binding model, respectively. All calculated F-ratios were greater than 1 (between 6.13 and 275.29), signifying that the bivalent ligand binding model more accurately described the binding data.

For refolded Cα3, SPR assays were also carried out at 25 ºC. The A59 antibody (BD-Pharmingen; No. 555685) that recognizes the D2 domain of FcαRI was diluted to 10 μg/mL in 10 mM sodium acetate buffer, pH 4.5, injected at 5 μL/min, and immobilized to ~3000 response units (RU) on a CM5 chip using standard random-amine chemistry. Baculovirus-expressed FcαRI ectodomain, diluted to 20 μg/ml in 0.02 M Tris-HCl, pH 7.4, 0.15 M NaCl, was captured until 150-200 RU was achieved. For equilibrium binding experiments, 30 μL aliquots of three-fold serial dilutions of Cα3 in degassed TBS-P (0.02 M Tris-HCl pH 7.4, 0.15 M NaCl, 0.005%

Surfactant P20) were injected at 5 μL/min at concentrations between 950 pM and 694.2 nM. Equilibrium binding curve alignment and subtraction of a buffer blank injection were performed with BIAeval 4.1 software (GE Healthcare).

Structure Alignment

Fcα C_H2 (Cα2) and C_H3 (Cα3) domains were defined as residues Cys242–Gly342 and residues Asn343–Lys450, respectively. The backbone of Fcα Cα3 (PDB ID: 1OW0) (6) was aligned with Fcα Cα3 (PDB ID: 2QEJ) (7), and with chicken IgY-Fc C_H4 (Cυ4) residues Tyr459-Lys564 (PDB ID: 2W59) (8). Backbone alignments and figures were generated using the program PyMOL (DeLano Scientific, San Francisco, CA).

Supplementary Figures

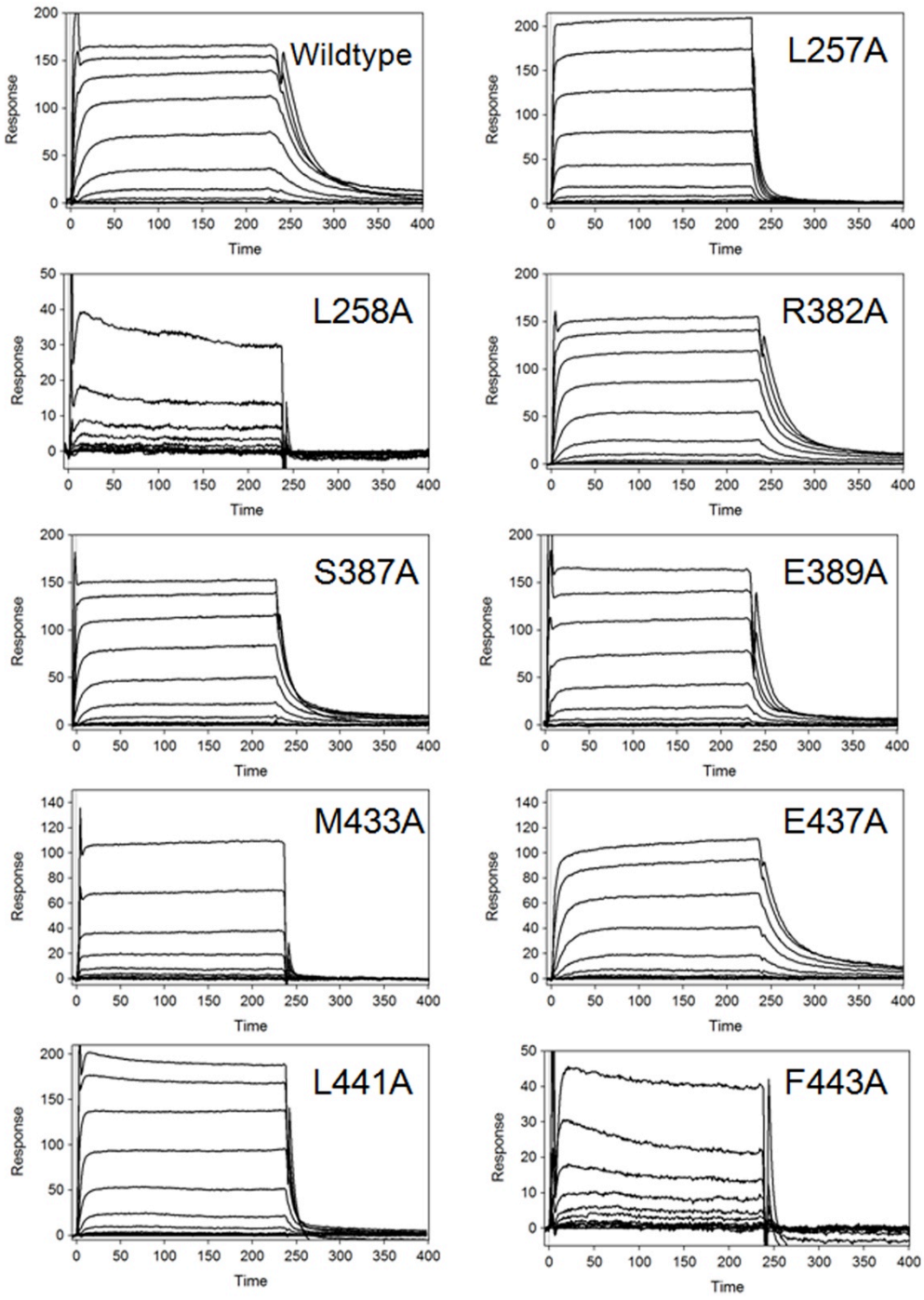

Figure S1. Representative equilibrium SPR sensorgrams of soluble FcαRI ectodomain binding to immobilized Fcα variants.

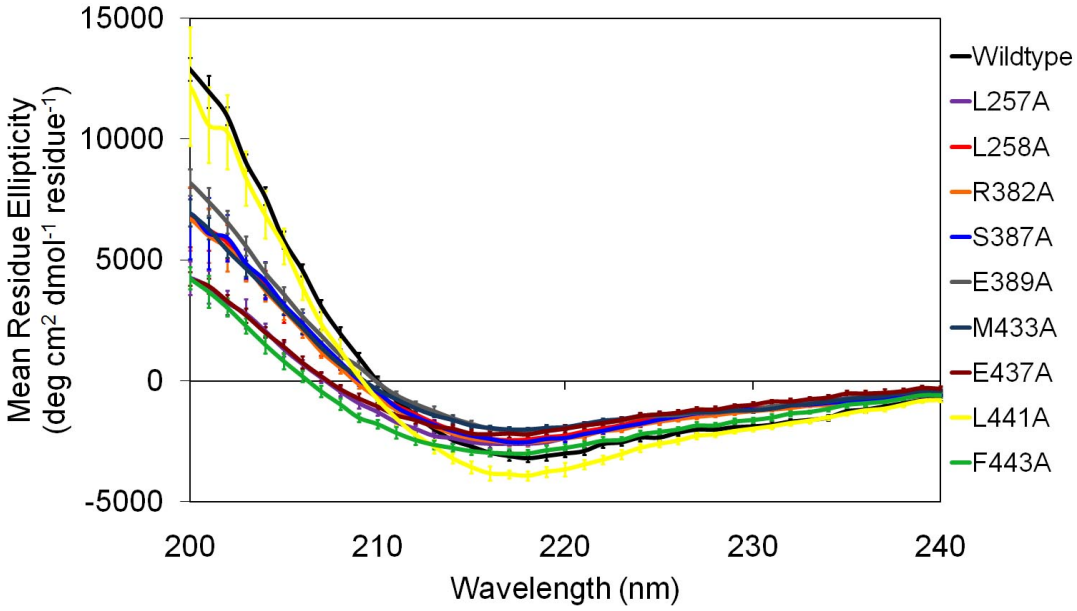

Figure S2. Far-UV CD wavelength spectra of Fcα variants.

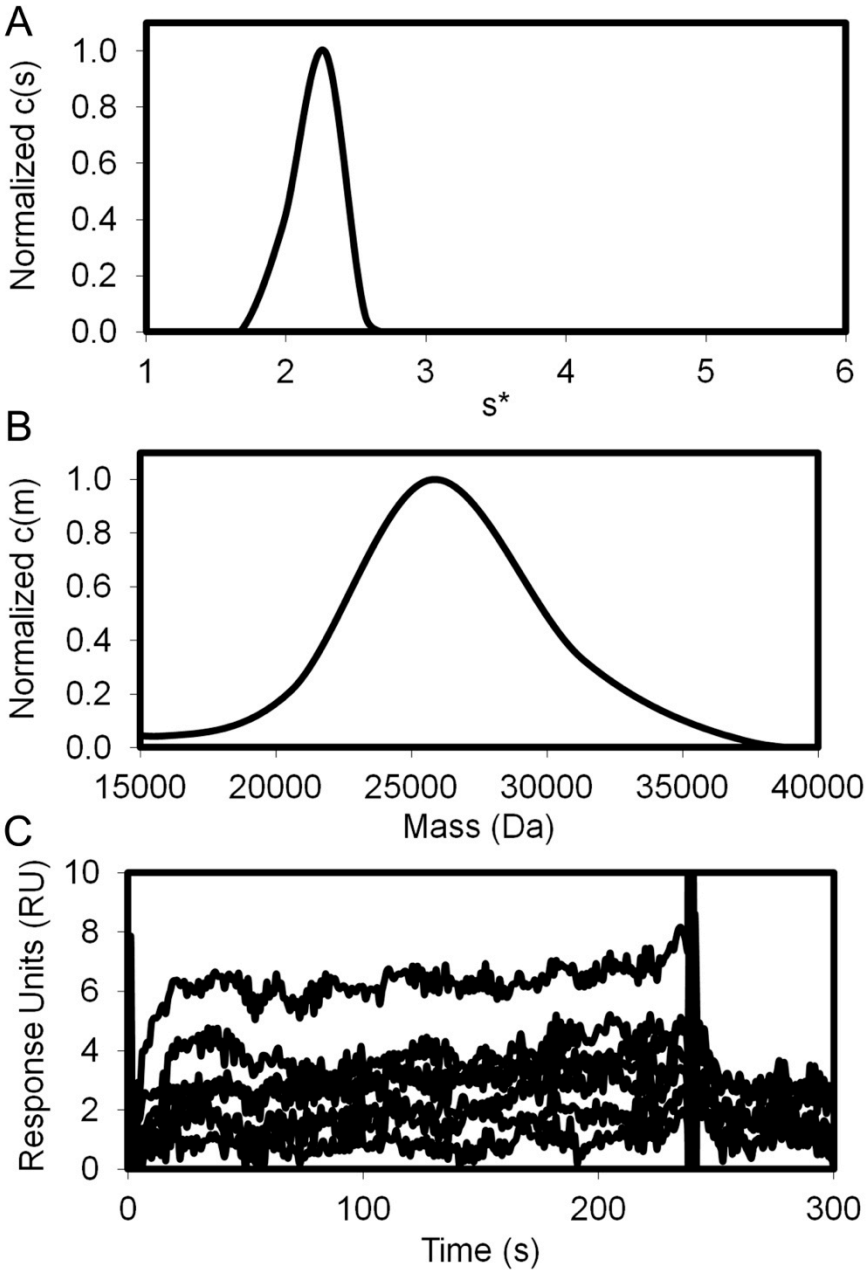

Figure S3. A-B) Refolded purified Cα3 forms a non-covalent homodimer in solution, based on sedimentation velocity analytical ultracentrifugation. Panel A shows the sedimentation coefficient distribution, revealing a single species with the predicted mass of a dimer (panel B). C) Cα3 analyte exhibits very low binding levels to captured FcαRI, indicating that the Cα2 is important in stable complex formation with FcαRI.

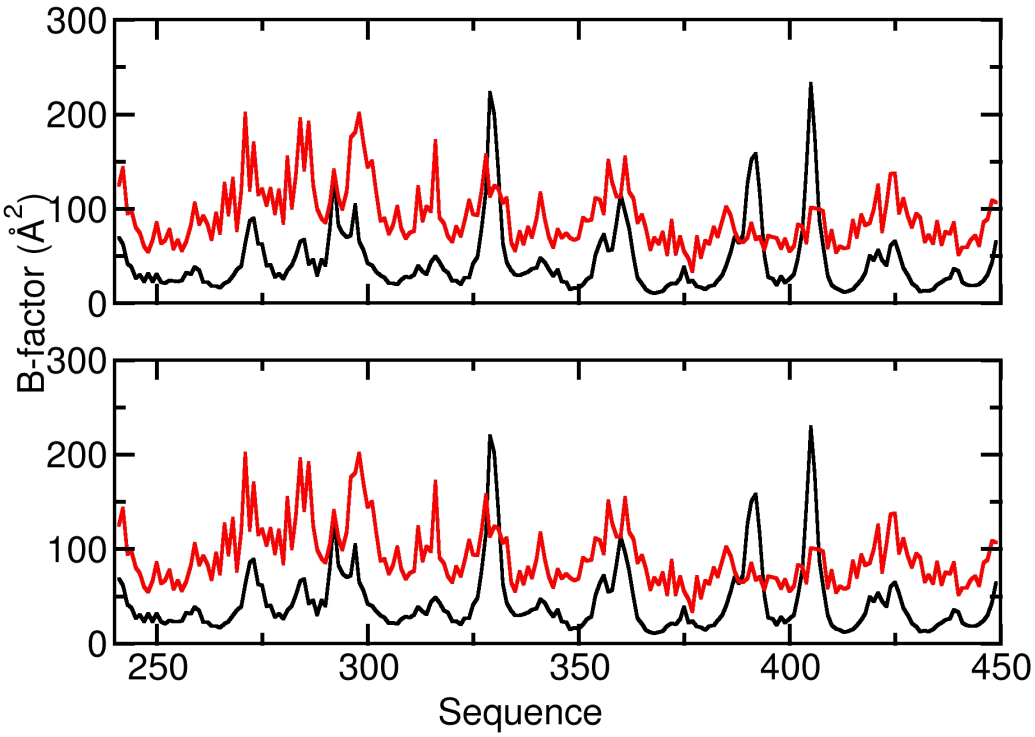

Figure S4. Experimental and computational B-factors of Fcα heavy chains in the 2:1 FcαRI:Fcα complex: Computational (black) and experimental (red) B-factor profiles for each Fcα heavy chain in the 2:1 FcαRI:Fcα complex are shown in the upper and lower panel, respectively. Experimental B-factors were taken from PDB 1OW0.

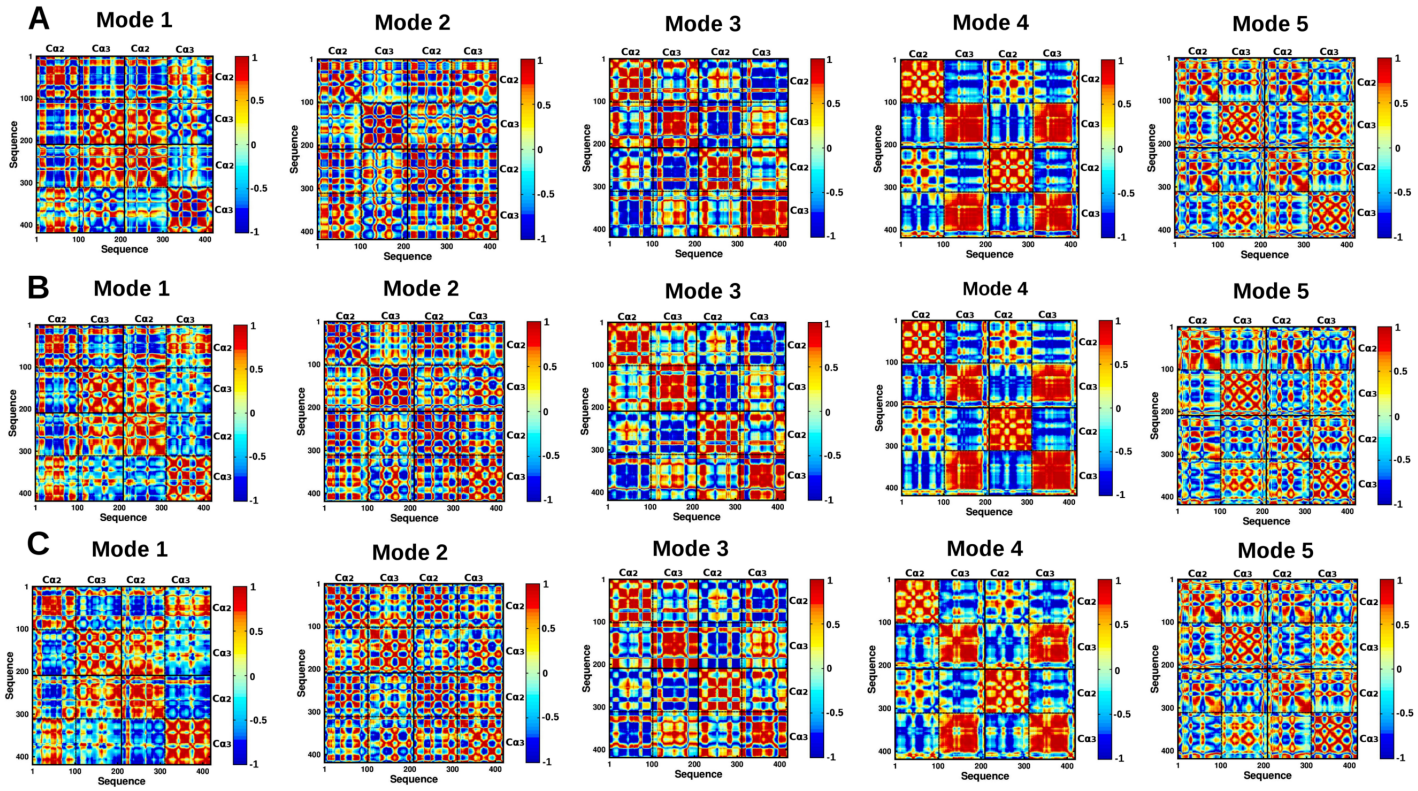

Figure S5. Directional correlation maps of Fcα amino acids in the five highest ranked PC modes for the A) Unliganded Fcα; B) FcαRI:Fcα 1:1 complex; C) FcαRI:Fcα 2:1 complex.

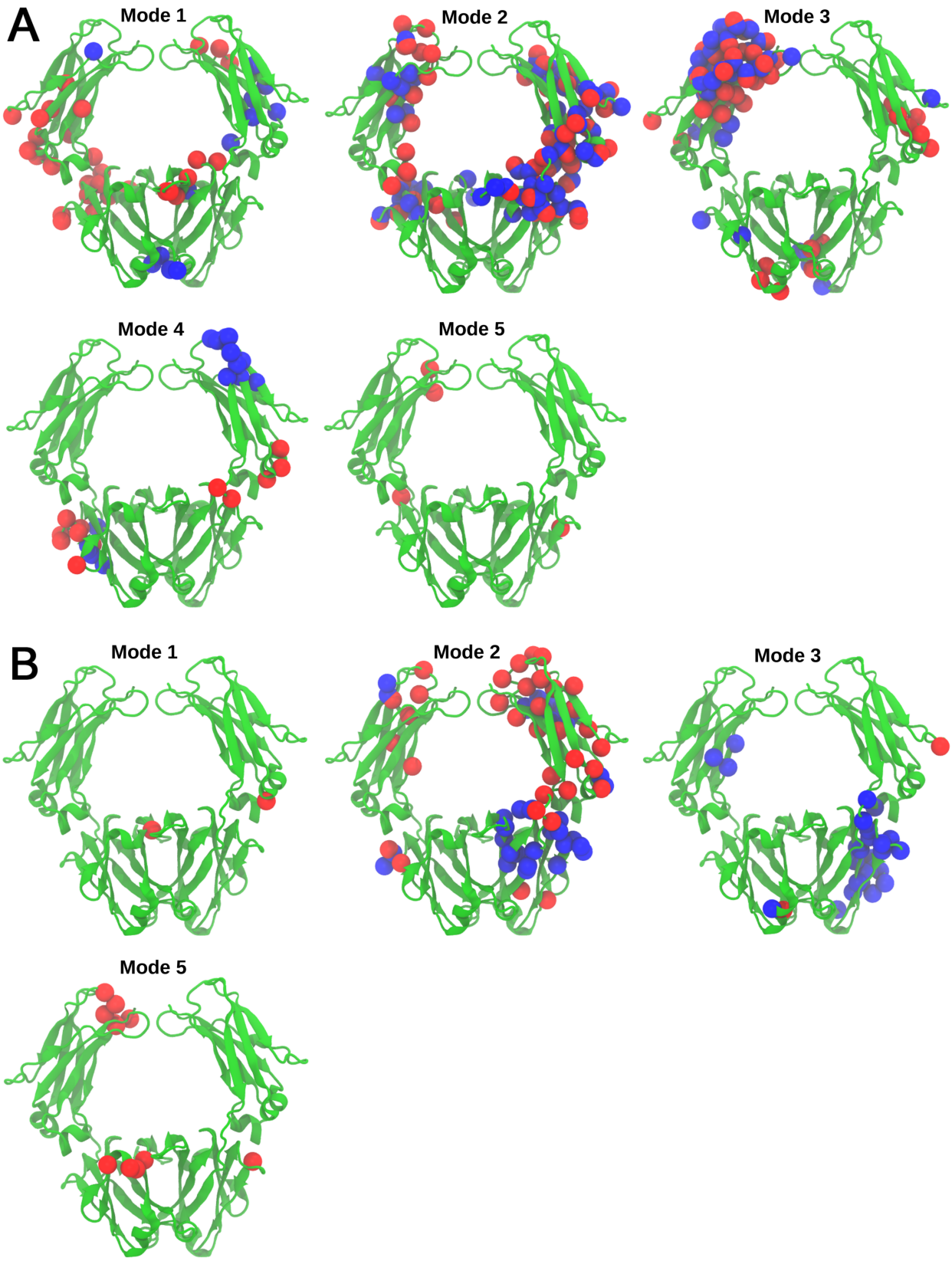
A
Mode 1
Mode 2
Mode 3
Mode 4
Mode 5
B
Mode 1
Mode 2
Mode 3
Mode 5

Figure S6. Fcα residue pairs that mediate ligand-induced long-distance communication.
A) Structural representation of intersubunit residue pairs which switch from weak directional correlation in the unliganded Fcα to strong correlation (blue spheres) or anticorrelation (red spheres) in the 1:1 and 2:1 FcαRI:Fcα complexes. The five panels indicate the residue pairs for the five highest ranked PC modes. The detailed list of residue pairs is provided in Supplementary Table S3. B) Structural representation of intersubunit residue pairs which switch from strong correlation, shown using red spheres (or anticorrelation, shown using blue spheres) in unliganded Fcα to strong anticorrelation (correlation) in the 2:1 complex. Mode 4 does not include such residue pairs. The detailed list of residue pairs is provided in Supplementary Table S4.

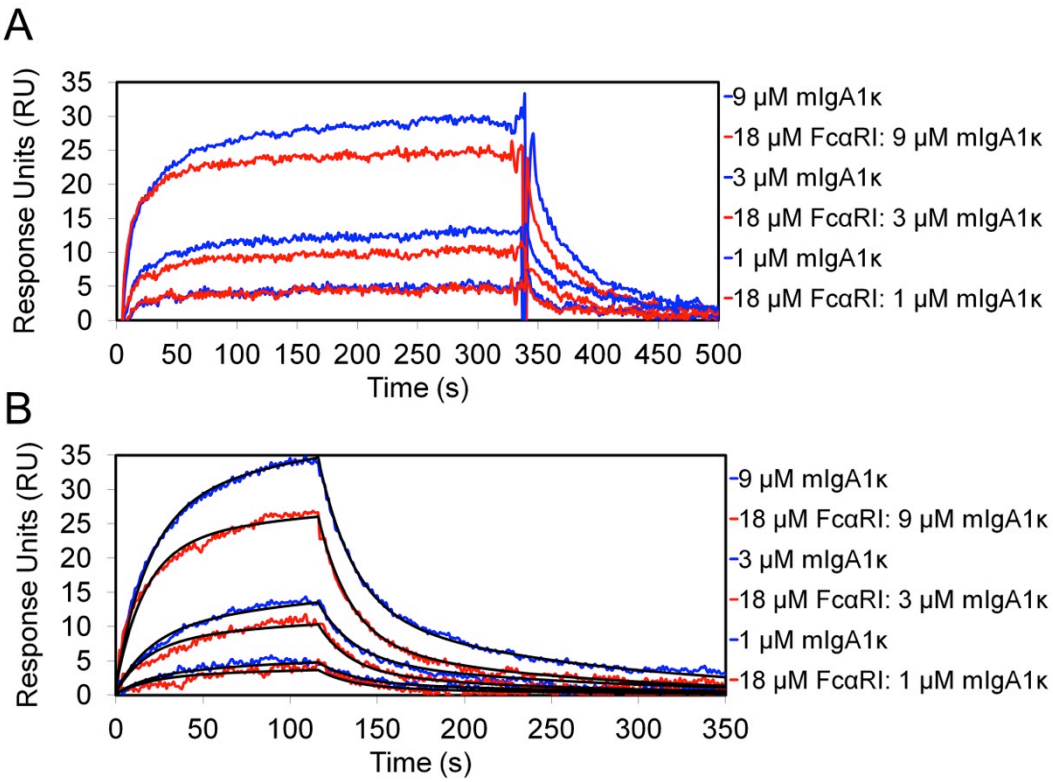

Figure S7. Sensorgrams displaying HAA ligand binding to mIgA1κ in the presence or absence of FcαRI. A) SPR data collected at 5 μl/minute. B) SPR data collected at 30 μl/minute, with the bivalent analyte fits superimposed in black.

Supplementary Tables

Table S1. CDSSTR analysis of the secondary structure content of wildtype and mutant Fcα variants revealed that alanine mutations did not alter the secondary structure content.

Fcα	Helix	Sheet	Turns	Unordered	Total	r.m.s.d.
Wildtype	7%	41%	22%	28%	98%	0.032
L257A	6%	40%	22%	31%	99%	0.070
L258A	6%	41%	23%	30%	100%	0.081
R382A	5%	42%	22%	30%	99%	0.073
S387A	5%	42%	22%	31%	100%	0.092
E389A	7%	41%	21%	29%	98%	0.032
M433A	7%	39%	22%	31%	99%	0.027
E437A	6%	41%	21%	30%	98%	0.041
L441A	5%	43%	22%	29%	99%	0.068
F443A	7%	39%	23%	30%	99%	0.045

Table S2. Binding interface properties of alanine-scanning Fcα mutants. Experimental ΔΔG values of energetic hotspot residues did not strongly correlate with the contribution to the binding surface or the percent buried surface area.

Fcα	Location	% Binding Surface[a]	BSA (Å^2)[b]	% Buried[b]	Experimental ΔΔG (kcal/mol)
R382	C strand	1%	5.83	20%	0.18
E437	FG loop	2%	13.73	50%	0.19
S387	CC' loop	10%	68.76	70%	0.27
E389	CC' loop	5%	33.43	40%	1.09
L441	FG loop	12%	44.30	60%	1.21
L257	AB helix/loop	8%	55.22	100%	2.34
M433	G strand	6%	48.42	100%	2.49
F443	F strand	5%	35.89	90%	2.93
L258	AB helix/loop	10%	77.61	90%	3.44

[a]from CNS analysis of FcαRI : Fcα complex (9)
[b]from PISA analysis of FcαRI : Fcα complex (10)

Table S3. Long-distance communication induced by receptor binding. Pairs of amino acids in distinct Fcα subunits, separated by at least 30 Å, which switch from weak directional correlation in the free Fcα to strong correlation in the 1:1 and 2:1 complexes (see Methods).

Mode	Correlated residue pairs				Anti-correlated residue pairs			
	residue	correlation in 2:1 complex	correlation in 1:1 complex	correlation in free Fcα	residue	correlation in 2:1 complex	correlation in 1:1 complex	correlation in free Fcα
1	292-413	0.9420	0.7180	0.0390	265-293	-0.9328	-0.6003	-0.1872
	294-413	0.9305	0.6367	-0.0363	265-294	-0.9716	-0.7050	-0.1666
	353-264	0.9326	0.7618	0.1684	265-302	-0.9666	-0.9085	0.0153
	353-290	0.9009	0.7670	0.1220	265-303	-0.9602	-0.9242	-0.1650
	353-291	0.9245	0.7697	0.1278	285-302	-0.9575	-0.7561	-0.1985
	353-307	0.9389	0.7988	0.1501	306-302	-0.9064	-0.7954	0.0017
	353-309	0.9447	0.8397	0.1054	308-302	-0.9409	-0.8992	0.0793
	353-310	0.9377	0.8119	0.0637	309-300	-0.9486	-0.7615	-0.1606
	354-252	0.9825	0.7588	0.1898	313-412	-0.9005	-0.6851	-0.1584
	359-252	0.9611	0.6169	0.0174	314-412	-0.9029	-0.7749	-0.0742
	362-252	0.9173	0.7103	0.1860	316-412	-0.9314	-0.7729	-0.0684
					317-412	-0.9249	-0.7713	-0.0386
					339-403	-0.9893	-0.8415	0.1715
					341-405	-0.9618	-0.6062	0.1660
					342-402	-0.9415	-0.6227	0.1444
					342-403	-0.9555	-0.7864	0.1245
					342-404	-0.9316	-0.6117	0.0155
					342-405	-0.9622	-0.6328	0.0700
					343-405	-0.9543	-0.6071	0.1185
					344-411	-0.9239	-0.6383	-0.0452
					345-411	-0.9553	-0.6427	-0.0455
					346-378	-0.9373	-0.7895	0.0725

					346-411	-0.9860	-0.6654	-0.1280
					375-377	-0.9542	-0.6713	0.0023
					408-402	-0.9746	-0.8540	-0.1975
					438-378	-0.9448	-0.7343	0.1973
					438-411	-0.9829	-0.6049	-0.0533
					440-412	-0.9647	-0.7193	-0.1635
					441-412	-0.9213	-0.6336	-0.1135
2	248-405	0.9816	0.7396	0.1806	248-367	-0.9450	-0.6570	-0.1335
	265-288	0.9699	0.6890	0.0090	248-385	-0.9190	-0.6695	-0.0100
	265-308	0.9492	0.7999	0.1491	248-386	-0.9455	-0.6893	-0.0003
	267-292	0.9986	0.9473	-0.1972	248-418	-0.9369	-0.6523	-0.0839
	267-305	0.9292	0.9251	-0.1709	248-419	-0.9670	-0.6941	-0.1070
	267-306	0.9159	0.9469	-0.1487	248-428	-0.9887	-0.7310	-0.1519
	268-293	0.9480	0.9053	-0.0541	248-429	-0.9852	-0.7161	-0.0568
	275-292	0.9094	0.8374	0.0645	248-430	-0.9688	-0.6707	0.0127
	275-294	0.9808	0.7621	0.0030	248-449	-0.9005	-0.6495	-0.1919
	275-295	0.9841	0.7216	-0.0859	249-246	-0.9992	-0.7601	-0.1437
	275-305	0.9910	0.8427	0.1357	249-247	-0.9598	-0.6438	0.1149
	279-287	0.9577	0.6784	0.1920	249-324	-0.9291	-0.6339	-0.0617
	292-265	0.9177	0.6387	0.0476	249-330	-0.9790	-0.8181	-0.1761
	304-291	0.9550	0.6719	-0.0288	249-331	-0.9882	-0.7598	-0.0969
	304-292	0.9537	0.7224	0.0472	249-332	-0.9894	-0.7092	-0.0392
	304-294	0.9413	0.6044	-0.0832	249-333	-0.9854	-0.6950	-0.0183
	304-304	0.9209	0.6022	0.0062	249-334	-0.9712	-0.6502	0.0493
	304-305	0.9908	0.6973	0.0207	249-353	-0.9584	-0.8143	0.0279
	304-306	0.9733	0.7401	0.0364	249-354	-0.9502	-0.8546	-0.1234
	305-290	0.9146	0.6910	0.0057	249-358	-0.9547	-0.8661	-0.1730
	344-341	0.9934	0.6037	0.1845	249-359	-0.9645	-0.8674	-0.0932
	346-321	0.9582	0.6075	0.1983	249-360	-0.9530	-0.8657	-0.1597
	374-340	0.9986	0.6588	0.1982	249-361	-0.9778	-0.8626	-0.0601
	375-434	0.9499	0.6847	0.1917	249-362	-0.9798	-0.8580	0.1200

	401-282	0.9685	0.6573	0.1719	249-450	-0.9680	-0.8398	0.1696
	406-281	0.9013	0.6059	0.1561	252-353	-0.9395	-0.8532	-0.1822
	434-407	0.9753	0.7667	-0.0665	253-450	-0.9314	-0.8480	-0.1037
	434-408	0.9629	0.7011	-0.1889	254-353	-0.9386	-0.9150	-0.0938
	435-407	0.9614	0.9972	-0.0756	254-354	-0.9261	-0.8967	-0.0996
	435-408	0.9769	0.9949	-0.1932	258-353	-0.9329	-0.9650	-0.1541
	437-251	0.9255	0.7758	0.1551	258-354	-0.9345	-0.9650	-0.1914
	437-253	0.9517	0.7830	0.1361	266-335	-0.9331	-0.8159	-0.1786
	437-256	0.9251	0.7190	0.1188	266-336	-0.9107	-0.6616	0.0200
	437-257	0.9111	0.7116	0.0934	267-250	-0.9133	-0.7725	-0.0973
	437-285	0.9145	0.8378	0.1395	267-318	-0.9441	-0.9400	-0.0696
	437-311	0.9001	0.7237	0.0944	267-319	-0.9285	-0.9305	-0.0522
	437-312	0.9381	0.7698	0.1165	267-320	-0.9810	-0.9807	0.0554
	437-313	0.9647	0.8398	0.1717	267-321	-0.9491	-0.9600	0.1337
	437-344	0.9377	0.8358	0.1832	267-338	-0.9479	-0.9436	0.1340
	437-345	0.9581	0.7889	0.1204	267-339	-0.9944	-0.9953	-0.0339
	437-346	0.9530	0.7561	0.0524	267-340	-0.9847	-0.9707	-0.1284
	437-347	0.9566	0.7951	0.0604	267-341	-0.9807	-0.9525	-0.1828
	437-371	0.9646	0.8379	0.0186	268-283	-0.9460	-0.9565	0.0198
	437-374	0.9466	0.7607	0.0081	268-318	-0.9557	-0.9100	-0.1711
	437-375	0.9573	0.7522	0.0039	268-319	-0.9630	-0.9230	-0.1556
	437-376	0.9785	0.8243	0.0760	268-320	-0.9503	-0.8311	0.1788
	437-377	0.9880	0.8492	0.0768	268-340	-0.9424	-0.8619	-0.0940
	437-411	0.9158	0.6942	-0.1597	268-341	-0.9201	-0.8523	-0.1707
	437-438	0.9932	0.7800	0.0840	271-321	-0.9193	-0.8091	-0.1463
	437-439	0.9945	0.7879	0.0994	273-321	-0.9027	-0.8104	-0.1554
	437-440	0.9993	0.7822	0.1083	275-283	-0.9281	-0.8351	-0.1112
	437-441	0.9967	0.8086	0.1674	275-320	-0.9414	-0.8824	-0.0743
	438-250	0.9812	0.6258	0.0548	275-321	-0.9174	-0.8390	0.0248
	438-317	0.9790	0.6344	0.0373	302-282	-0.9045	-0.6074	0.0304

	438-318	0.9982	0.7440	0.1865	303-282	-0.9055	-0.6654	0.0057
	438-340	0.9823	0.7431	0.1797	327-251	-0.9675	-0.6962	-0.1171
	438-341	0.9825	0.6758	0.1032	327-253	-0.9551	-0.6946	-0.1865
	439-320	0.9847	0.7164	0.0830	327-378	-0.9326	-0.6662	0.0067
	439-321	0.9593	0.7429	0.1851	327-379	-0.9589	-0.6563	0.0321
	439-339	0.9603	0.7164	0.0611	327-380	-0.9962	-0.7806	-0.1251
	440-320	0.9923	0.7698	0.0619	327-381	-0.9953	-0.8130	-0.1654
	440-321	0.9897	0.8001	0.1640	327-397	-0.9892	-0.8036	-0.1427
	440-339	0.9536	0.7578	0.0425	327-398	-0.9250	-0.6862	-0.0167
					327-415	-0.9570	-0.8181	-0.1605
					327-434	-0.9904	-0.7000	-0.0766
					327-435	-0.9751	-0.6896	-0.0965
					327-443	-0.9701	-0.6625	-0.1121
					327-445	-0.9542	-0.7657	-0.1424
					328-315	-0.9004	-0.6432	0.1386
					328-378	-0.9292	-0.7136	-0.0967
					328-379	-0.9465	-0.6966	-0.0748
					328-398	-0.9040	-0.7152	-0.1296
					328-434	-0.9786	-0.7359	-0.1841
					328-436	-0.9268	-0.6464	-0.0721
					328-442	-0.9262	-0.6269	-0.1308
					347-293	-0.9284	-0.6896	-0.1822
					372-290	-0.9132	-0.6228	-0.1724
					372-291	-0.9234	-0.6262	-0.1545
					372-292	-0.9217	-0.6241	-0.1589
					381-279	-0.9019	-0.6209	-0.1977
					434-425	-0.9383	-0.8312	-0.1602
					435-243	-0.9571	-0.9592	0.1681
					435-245	-0.9095	-0.9239	0.1977
					435-425	-0.9498	-0.9770	-0.1524

					435-450	-0.9643	-0.9743	-0.0515
					436-296	-0.9164	-0.9718	-0.1129
					436-297	-0.9362	-0.9674	-0.1604
					436-298	-0.9457	-0.9799	-0.1027
					436-299	-0.9414	-0.9977	0.1923
					436-302	-0.9707	-0.9993	0.1389
					436-303	-0.9792	-0.9979	0.0810
					436-304	-0.9641	-0.9955	0.0587
					437-270	-0.9139	-0.8363	-0.1006
					437-271	-0.9441	-0.8526	-0.1359
					437-272	-0.9587	-0.8586	-0.1398
					437-273	-0.9714	-0.8656	-0.1599
					437-278	-0.9308	-0.8371	-0.1365
					438-299	-0.9151	-0.6393	-0.0232
					438-302	-0.9171	-0.6634	-0.0912
					438-303	-0.9195	-0.7000	-0.1496
					438-304	-0.9458	-0.7240	-0.1743
					439-291	-0.9612	-0.6496	0.1013
					439-292	-0.9712	-0.6803	0.0688
					439-293	-0.9681	-0.7576	-0.1636
					439-294	-0.9923	-0.6114	0.0727
					439-295	-0.9869	-0.6285	0.0060
					440-291	-0.9227	-0.7252	0.1303
					440-292	-0.9413	-0.7482	0.0965
					440-293	-0.9818	-0.8293	-0.1339
					440-294	-0.9975	-0.6953	0.1023
					440-295	-0.9954	-0.7134	0.0364
					440-297	-0.9515	-0.6020	0.1753
					443-422	-0.9007	-0.6091	0.0553
3	249-365	0.9472	0.7900	0.1679	243-311	-0.9845	-0.8131	-0.1361

	250-420	0.9509	0.6131	0.1313	244-311	-0.9716	-0.8663	-0.1666
	250-421	0.9112	0.9273	-0.0265	245-311	-0.9799	-0.8060	-0.1565
	271-425	0.9667	0.6561	-0.1618	246-311	-0.9669	-0.8349	-0.1552
	272-425	0.9741	0.6719	-0.1251	247-311	-0.9660	-0.7559	-0.1864
	273-425	0.9660	0.7166	-0.0227	265-311	-0.9276	-0.7740	-0.1565
	274-425	0.9860	0.8026	0.0296	266-311	-0.9591	-0.8010	-0.0697
	275-425	0.9844	0.8109	0.0294	267-311	-0.9675	-0.8304	-0.1136
	276-425	0.9460	0.8474	0.1565	268-311	-0.9698	-0.8518	-0.0872
	277-425	0.9544	0.8292	0.0856	269-311	-0.9737	-0.8505	-0.1262
	278-425	0.9025	0.8633	0.1917	270-311	-0.9788	-0.8714	-0.1372
	279-425	0.9122	0.8521	0.1227	271-311	-0.9696	-0.9165	-0.1319
	291-425	0.9541	0.8681	0.0731	272-311	-0.9717	-0.9252	-0.1338
	292-425	0.9718	0.8727	0.0245	273-311	-0.9544	-0.9459	-0.1175
	293-425	0.9287	0.7094	-0.1708	273-314	-0.9033	-0.6534	-0.1587
	294-425	0.9655	0.7413	-0.1364	274-311	-0.9595	-0.8755	0.0565
	295-425	0.9397	0.7373	-0.1161	274-314	-0.9492	-0.7155	-0.1451
	296-425	0.9518	0.7486	-0.0937	275-311	-0.9605	-0.8632	0.0734
	299-425	0.9163	0.9000	0.1296	275-314	-0.9428	-0.7196	-0.1382
	301-425	0.9684	0.7080	-0.1447	276-311	-0.9087	-0.8695	0.0777
	302-425	0.9658	0.6625	-0.1897	277-311	-0.9226	-0.8530	0.0978
	304-425	0.9567	0.7107	-0.1437	277-314	-0.9349	-0.7406	-0.1849
	306-425	0.9449	0.7712	-0.0973	279-314	-0.9202	-0.7506	-0.1949
	320-284	0.9384	0.8234	0.1653	285-367	-0.9959	-0.8891	-0.0403
	323-425	0.9221	0.6731	-0.1708	291-311	-0.9472	-0.7769	0.1546
	324-425	0.9071	0.7080	-0.0640	292-311	-0.9769	-0.7810	0.1412
	325-425	0.9363	0.7269	-0.0475	293-311	-0.9668	-0.8499	-0.0152
	326-425	0.9127	0.7475	0.0315	294-311	-0.9864	-0.8214	0.0322
	327-425	0.9432	0.7510	0.0218	295-311	-0.9617	-0.8616	-0.0598
	328-425	0.9285	0.7450	0.0605	296-311	-0.9651	-0.8724	-0.0882
	329-425	0.9392	0.6971	-0.0241	297-311	-0.9028	-0.8989	-0.1842

	330-425	0.9308	0.6660	-0.0791	300-311	-0.9959	-0.8936	-0.1350
	331-425	0.9016	0.6712	-0.0204	301-311	-0.9740	-0.9054	-0.1612
	332-425	0.9163	0.6004	-0.1216	302-311	-0.9856	-0.9084	-0.1261
	333-425	0.9058	0.6527	-0.0844	303-311	-0.9762	-0.8767	-0.0966
	384-419	0.9210	0.6509	0.1906	304-311	-0.9704	-0.8721	-0.0423
	441-419	0.9871	0.7197	-0.0096	305-311	-0.9710	-0.8387	-0.0336
	441-420	0.9190	0.8571	0.1405	306-311	-0.9534	-0.8087	0.0619
					307-311	-0.9463	-0.7647	0.0352
					318-353	-0.9412	-0.9094	-0.0452
					319-352	-0.9431	-0.7806	0.1902
					323-311	-0.9001	-0.8101	0.0583
					325-311	-0.9048	-0.8646	0.0332
					325-313	-0.9104	-0.6046	-0.1301
					325-314	-0.9196	-0.6084	-0.0762
					326-314	-0.9225	-0.6494	-0.1586
					327-311	-0.9064	-0.9037	-0.0012
					327-314	-0.9355	-0.6624	-0.1596
					329-311	-0.9031	-0.9287	-0.0731
					329-314	-0.9308	-0.6105	-0.1408
					334-311	-0.9246	-0.8718	-0.0844
					335-311	-0.9075	-0.8460	-0.0689
					336-311	-0.9488	-0.7931	-0.1560
					337-311	-0.9190	-0.7303	-0.1674
					353-321	-0.9082	-0.8229	-0.0279
					427-311	-0.9384	-0.8010	-0.1878
					448-309	-0.9242	-0.7733	-0.1953
					449-307	-0.9439	-0.7157	-0.1882
					449-309	-0.9698	-0.6956	0.0312
					450-311	-0.9949	-0.7791	-0.0651
4	346-331	0.9721	0.9496	0.1647	387-314	-0.9172	-0.6968	-0.1889

	444-327	0.9569	0.9754	0.1559	387-316	-0.9463	-0.7049	-0.1993
	444-328	0.9156	0.9532	0.0591	387-317	-0.9255	-0.6657	-0.0931
	444-329	0.9343	0.9673	0.0639	439-343	-0.9070	-0.8652	0.1242
	444-330	0.9629	0.9906	0.1924	440-343	-0.9610	-0.9005	0.0389
	445-279	0.9080	0.9426	-0.0046	440-344	-0.9590	-0.9521	-0.1533
	445-325	0.9098	0.9089	-0.0078	441-343	-0.9680	-0.8954	0.1369
	445-326	0.9718	0.9546	-0.1456	441-344	-0.9560	-0.9558	-0.1033
	445-331	0.9779	0.9675	-0.1233	443-343	-0.9493	-0.8710	-0.1293
	445-332	0.9697	0.9162	0.0660	444-344	-0.9568	-0.9631	-0.0817
	446-332	0.9430	0.8245	-0.1588				
	446-333	0.9641	0.8628	0.0529				
	446-334	0.9054	0.8164	0.1068				
5					244-443	-0.9850	-0.7724	-0.0025
					245-443	-0.9968	-0.7747	-0.1528
					437-443	-0.9315	-0.8805	-0.1535

Table S4. Effect of receptor binding on long-distance communication in Fcα. Pairs of amino acids in distinct Fcα subunits, separated by at least 30 Å, that undergo changes from strong directional correlation (anticorrelation) to strong anticorrelation (correlation) upon FcαRI binding.

Mode	Strong-negative to strong-positive				Strong-positive to strong-negative			
	residue	correlation in 2:1 complex	correlation in 1:1 complex	correlation in free Fc	residue	correlation in 2:1 complex	correlation in 1:1 complex	correlation in free Fc
1					398-316	-0.9210	0.5609	0.9794
2	276-291	0.9264	0.6142	-0.9984	249-447	-0.9329	-0.5001	0.9213
	276-292	0.9372	0.6736	-0.9989	266-351	-0.9334	-0.4825	0.9635
	276-293	0.9331	0.4956	-0.9606	268-281	-0.9623	-0.0786	0.9957
	276-294	0.9877	0.5373	-0.9948	271-281	-0.9286	0.1193	0.9260
	276-295	0.9875	0.4968	-0.9830	273-281	-0.9021	0.1474	0.9164
	276-303	0.9414	0.4797	-0.9453	276-250	-0.9197	-0.4196	0.9359
	276-304	0.9716	0.4955	-0.9533	276-283	-0.9108	-0.5905	0.9717
	276-305	0.9930	0.6246	-0.9932	276-317	-0.9699	-0.5462	0.9295
	277-291	0.9855	0.0832	-0.9778	276-318	-0.9883	-0.6824	0.9568
	277-292	0.9895	0.1606	-0.9743	276-319	-0.9836	-0.6589	0.9610
	277-294	0.9713	-0.0073	-0.9670	276-320	-0.9594	-0.7712	0.9155
	277-295	0.9608	-0.0240	-0.9397	276-340	-0.9659	-0.7587	0.9277
	277-305	0.9728	0.0387	-0.9922	276-341	-0.9876	-0.7496	0.9153
	277-306	0.9435	0.0927	-0.9949	277-250	-0.9055	0.2900	0.9885
	441-349	0.9842	-0.0872	-0.9439	277-317	-0.9045	0.1631	0.9857
	441-370	0.9915	-0.0679	-0.9561	277-318	-0.9646	-0.0457	0.9763
	441-371	0.9763	-0.2027	-0.9490	277-319	-0.9512	-0.0195	0.9762

	441-377	0.9627	-0.2294	-0.9050	277-340	-0.9815	-0.1516	0.9439
	441-400	0.9481	-0.2132	-0.9323	277-341	-0.9927	-0.1038	0.9489
	441-413	0.9664	-0.1851	-0.9375	277-342	-0.9947	-0.1262	0.9123
	441-436	0.9069	-0.2524	-0.9089	277-343	-0.9642	0.0220	0.9222
	441-437	0.9197	-0.2899	-0.9143	277-344	-0.9634	0.1086	0.9226
	441-438	0.9629	-0.2787	-0.9128	442-267	-0.9506	-0.7068	0.9007
	441-439	0.9614	-0.2595	-0.9212	442-268	-0.9108	-0.5609	0.9855
	441-440	0.9367	-0.3096	-0.9332	442-269	-0.9577	-0.6101	0.9612
	441-441	0.9143	-0.3078	-0.9347	442-270	-0.9413	-0.5739	0.9809
	441-444	0.9407	-0.1850	-0.9316	442-271	-0.9620	-0.5903	0.9709
	442-313	0.9184	0.4338	-0.9822	442-272	-0.9703	-0.6009	0.9651
	442-314	0.9459	0.5820	-0.9054	442-273	-0.9769	-0.6092	0.9590
	442-347	0.9856	0.7299	-0.9180	442-274	-0.9945	-0.6559	0.9209
	442-348	0.9154	0.6720	-0.9326	442-275	-0.9963	-0.6771	0.9052
	442-349	0.9017	0.7529	-0.9660	442-276	-0.9981	-0.6528	0.9286
	442-371	0.9932	0.6629	-0.9655	442-277	-0.9989	-0.6427	0.9385
	442-372	0.9270	0.6319	-0.9012	442-278	-0.9784	-0.5733	0.9740
	442-376	0.9983	0.6723	-0.9109	442-279	-0.9140	-0.5883	0.9770
	442-377	0.9950	0.6330	-0.9344	442-301	-0.9794	-0.6412	0.9080
	442-378	0.9186	0.4968	-0.9652	442-327	-0.9179	-0.4911	0.9850
	442-400	0.9957	0.6337	-0.9584	442-328	-0.9132	-0.4801	0.9833
	442-411	0.9781	0.6149	-0.9058	443-266	-0.9019	0.1972	0.9432
	442-436	0.9199	0.5599	-0.9604	443-267	-0.9731	0.3897	0.9663
	442-437	0.9463	0.5601	-0.9598	443-268	-0.9271	0.2733	0.9194
	442-438	0.9873	0.6185	-0.9426	443-269	-0.9046	0.3519	0.9507
	442-439	0.9802	0.6331	-0.9523	443-278	-0.9353	0.2552	0.9079
	442-440	0.9828	0.5889	-0.9642	443-279	-0.9950	0.2311	0.9089

	442-441	0.9549	0.5792	-0.9731				
	442-442	0.9200	0.5335	-0.9769				
	442-444	0.9062	0.6388	-0.9753				
3	247-423	0.9076	-0.8170	-0.9439	424-285	-0.9992	0.5930	0.9150
	249-423	0.9193	-0.6611	-0.9800	424-286	-0.9919	0.6250	0.9545
	265-423	0.9109	-0.8756	-0.9286				
	423-254	0.9136	-0.9299	-0.9961				
	423-342	0.9031	-0.9378	-0.9888				
	423-344	0.9054	-0.9258	-0.9913				
	423-382	0.9098	-0.8725	-0.9887				
	423-383	0.9347	-0.8795	-0.9889				
	423-384	0.9635	-0.8791	-0.9769				
	423-385	0.9580	-0.8869	-0.9704				
	423-386	0.9772	-0.8750	-0.9163				
	423-387	0.9659	-0.8961	-0.9494				
	423-388	0.9608	-0.8720	-0.9798				
	423-389	0.9168	-0.9006	-0.9886				
	423-430	0.9595	-0.8475	-0.9136				
	423-431	0.9451	-0.8485	-0.9375				
	423-433	0.9315	-0.8903	-0.9853				
	423-434	0.9168	-0.8906	-0.9904				
	423-435	0.9112	-0.9051	-0.9937				
	423-436	0.9040	-0.9024	-0.9919				
	423-439	0.9019	-0.9303	-0.9980				
	423-441	0.9109	-0.9139	-0.9897				
	423-442	0.9070	-0.9257	-0.9956				
	423-443	0.9023	-0.9044	-0.9887				
5					243-442	-0.9390	-0.5455	0.9620
					244-442	-0.9017	-0.2047	0.9481
					270-442	-0.9858	-0.3553	0.9794

		271-442	-0.9285	0.3097	0.9606
		272-442	-0.9886	0.1247	0.9827
		273-442	-0.9324	0.6893	0.9765
		391-442	-0.9385	-0.5798	0.9154
		394-442	-0.9636	-0.6255	0.9018
		395-442	-0.9221	-0.6679	0.9130
		436-442	-0.9019	-0.9398	0.9615

Supplementary Movies

Note: As a guide to the eye, supplementary movies illustrating PC modes of 1:1 and 2:1 FcαRI-Fcα indicate the X-ray configuration of receptor molecules (yellow).

Movie SM1. Unliganded Fcα mode motion in PC mode 1

Movie SM2. 1:1 FcαRI-Fcα mode motion in PC mode 1

Movie SM3. 2:1 FcαRI-Fcα mode motion in PC mode 1

Movie SM4. Unliganded Fcα mode motion in PC mode 2

Movie SM5. 1:1 FcαRI-Fcα mode motion in PC mode 2

Movie SM6. 2:1 FcαRI-Fcα mode motion in PC mode 2

Movie SM7. Unliganded Fcα mode motion in PC mode 3

Movie SM8. 1:1 FcαRI-Fcα mode motion in PC mode 3

Movie SM9. 2:1 FcαRI-Fcα mode motion in PC mode 3

Movie SM10. Unliganded Fcα mode motion in PC mode 4

Movie SM11. 1:1 FcαRI-Fcα mode motion in PC mode 4

Movie SM12. 2:1 FcαRI-Fcα mode motion in PC mode 4

Movie SM13. Unliganded Fcα mode motion in PC mode 5

Movie SM14. 1:1 FcαRI-Fcα mode motion in PC mode 5

Movie SM15. 2:1 FcαRI-Fcα mode motion in PC mode 5

Supplementary References

1. Whitmore L & Wallace BA (2004) DICHROWEB, an online server for protein secondary structure analyses from circular dichroism spectroscopic data. *Nucleic acids research* 32(Web Server issue):W668-673.
2. Sreerama N & Woody RW (2000) Estimation of protein secondary structure from circular dichroism spectra: comparison of CONTIN, SELCON, and CDSSTR methods with an expanded reference set. *Analytical biochemistry* 287(2):252-260.
3. Conrady DG*, et al.* (2008) A zinc-dependent adhesion module is responsible for intercellular adhesion in staphylococcal biofilms. *Proc Natl Acad Sci U S A* 105(49):19456-19461.
4. Day YS, Baird CL, Rich RL, & Myszka DG (2002) Direct comparison of binding equilibrium, thermodynamic, and rate constants determined by surface- and solution-based biophysical methods. *Protein Sci* 11(5):1017-1025.
5. Herr AB, White CL, Milburn C, Wu C, & Bjorkman PJ (2003) Bivalent binding of IgA1 to FcalphaRI suggests a mechanism for cytokine activation of IgA phagocytosis. *J Mol Biol* 327(3):645-657.
6. Herr AB, Ballister ER, & Bjorkman PJ (2003) Insights into IgA-mediated immune responses from the crystal structures of human FcalphaRI and its complex with IgA1-Fc. *Nature* 423(6940):614-620.
7. Ramsland PA*, et al.* (2007) Structural basis for evasion of IgA immunity by Staphylococcus aureus revealed in the complex of SSL7 with Fc of human IgA1. *Proc Natl Acad Sci U S A* 104(38):15051-15056.
8. Taylor AI, Fabiane SM, Sutton BJ, & Calvert RA (2009) The crystal structure of an avian IgY-Fc fragment reveals conservation with both mammalian IgG and IgE. *Biochemistry* 48(3):558-562.
9. Brunger AT*, et al.* (1998) Crystallography & NMR system: A new software suite for macromolecular structure determination. *Acta Crystallogr D Biol Crystallogr* 54(Pt 5):905-921.
10. Krissinel E & Henrick K (2007) Inference of macromolecular assemblies from crystalline state. *J Mol Biol* 372(3):774-797.